第 36 卷第 5 期
2020 年 5 月

无 机 化 学 学 报
CHINESE JOURNAL OF INORGANIC CHEMISTRY

Vol.36 No.5
927-932

溶剂诱导的两例单核 Er^{3+}配合物的合成、晶体结构及磁性

郗 婧 麻秀芳 徐燕红 周惠良* 周钰婷 刘翔宇*
(宁夏大学化学化工学院,煤炭高效利用与绿色化工国家重点实验室,
国家级实验教学示范中心,银川 750021)

摘要: 通过调整溶剂组分的比例,成功合成了 2 例结构不同的单核 Er^{3+}配合物:$[Er(bpad)_3]\cdot CH_3OH\cdot H_2O$ (**1**)和$[Er(bpad)_2(H_2O)_2]NO_3\cdot 3H_2O$ (**2**)(Hbpad=N_3-苯甲酰吡啶基-2-羰基氨基酰腙)。在甲醇/水(2∶1,*V*/*V*)的混合溶剂中加入 $Er(NO_3)_3\cdot 6H_2O$、Hbpad 和三乙胺反应制得黄色晶体配合物 **1**。配合物 **2** 的合成方法与 **1** 相似,仅将溶剂组分甲醇和水的体积比调整为 1∶2。通过红外光谱、元素分析对 2 例配合物进行了表征。2 例配合物在空气中都有良好的稳定性,并在室温下均保持晶体的完整性。晶体结构分析表明,配合物 **1** 和 **2** 中的 Er^{3+}金属中心分别显示了九配位和八配位环境。配合物 **1** 中 Er^{3+}离子表现为单帽四方反棱柱构型,而配合物 **2** 中 Er^{3+}离子呈现了双帽三棱柱构型。此外,2 例配合物的直流和交流磁化率测试结果表明,**1** 和 **2** 在零场下均未展示出单分子磁体特征。

关键词: 铒配合物; 溶剂效应; 晶体结构; 磁性
中图分类号: O614.344 **文献标识码**: A **文章编号**: 1001-4861(2020)05-0927-06
DOI: 10.11862/CJIC.2020.103

Solvent-Induced Syntheses, Crystal Structures and Magnetic Properties of Two Mononuclear Er(Ⅲ) Complexes

XI Jing MA Xiu-Fang XU Yan-Hong ZHOU Hui-Liang* ZHOU Yu-Ting LIU Xiang-Yu*
(*State Key Laboratory of High-Efficiency Coal Utilization and Green Chemical Engineering, National Demonstration Center for Experimental Chemistry Education, College of Chemistry and Chemical Engineering, Ningxia University, Yinchuan* 750021, *China*)

Abstract: By adjusting the ratio of the solvent components, two mononuclear erbium complexes, $[Er(bpad)_3]\cdot CH_3OH\cdot H_2O$ (**1**) and $[Er(bpad)_2(H_2O)_2]NO_3\cdot 3H_2O$ (**2**) (Hbpad=N_3-benzoylpyridine-2-carboxamidrazone), have been successfully synthesized. In the mixure of methanol and water solvent (2∶1, *V*/*V*), yellow crystals of **1** were prepared by solution reaction of $Er(NO_3)_3\cdot 6H_2O$, Hbpad and triethylamine. Interestingly, complex **2** was obtained by the similar way of **1**, while the volume ratio of CH_3OH to H_2O is altered to be 1∶2. The resulting complexes were characterized by IR spectrum, elemental analysis. Two complexes are air stable, and can maintain the crystalline integrities at ambient conditions. Crystal structure analysis indicates that the Er(Ⅲ) ions in **1** and **2** present nona-coordinated and octa-coordinated environments in different coordination geometries, respectively. Monocapped square antiprism (C_{4v}) is formed in **1**, while biaugmented trigonal prism (C_{2v}) is observed in **2**. The direct-current (dc) and alternating-current (ac) magnetic susceptibilities of **1** and **2** have been analyzed as well. CCDC: 1478582, **1**; 1478579, **2**.

Keywords: erbium(Ⅲ) complex; solvent effect; crystal structure; magnetic property

收稿日期:2019-11-15。收修改稿日期:2020-03-13。
国家自然科学基金(No.21863009, 21463020),宁夏回族自治区国内一流学科建设项目(No.NXYLXK2017A04)和宁夏回族自治区大学生创新创业训练计划(No.2019107490041)资助。
*通信联系人。E-mail:xiangyuliu432@126.com,13995209835@163.com

After the discovery of the first single-ion magnet $[TbPc_2]^-$ (Pc^{2-}=pthalocyanine dianion)[1], lanthanide based complexes have gained momentum in the area of molecular magnetism as they exhibit slow relaxation of magnetization at low temperatures[2-6]. Thanks to their unquenched orbital angular momentum and inherent magnetic anisotropy, the number of lanthanide-based single-molecule magnets (SMMs) reported to-date is increasing exponentially[7-14]. Such molecules hold tremendous application potential in high-density data storage and/or quantum computation due to their magnetic moment bistability. By using geometric design principles to minimize electronic repulsions between the electron densities of the lanthanide ions and the ligands, researchers have prepared SMMs with extremely high barriers and magnetic hysteresis as compared to previous examples[15]. Especially, a breakthrough has been made by Layfield and co-workers in Dy-SIMs, exhibiting magnetic hysteresis at temperatures up to 80 K and a high effective energy barrier of 1 541 cm^{-1} [16]. While most examples of the rare-earth SMMs are based on the oblate terbium and dysprosium ions (and particularly the latter[17-19]), emerging work has revealed that prolate ions can also engender SMM behavior, with the erbium (Ⅲ) ion being the main choice for such systems[20-22]. The first reported erbium(Ⅲ) mononuclear SMM is the organometallic complex [(Cp)Er(COT)] (Cp=pentamethylcyclopentadienide; COT =cyclooctatetraenide), reported by Gao and co-workers, which exhibits two relaxation processes with energy barriers $\Delta E_{eff}/k_B$ of 197 and 323 K and a butterfly hysteresis loop as high as 5 K[23]. The lack of SMM behavior in the majority of the Er(Ⅲ) complexes and the presence of large T_B values in some other Er(Ⅲ) complexes have attracted our attention.

Existing researches point out that different environments of the magnetic centers generating various crystal fields usually bring about distinct dynamic magnetic relaxation processes; even subtle changes of the coordination pattern can drastically affect the overall magnetic properties of SMMs. It is well-known that the structural formation of a target complex is often perturbed by rational changes of the synthetic conditions such as solvent effect, pH, counterions[24-31]. Of particular concern is the tunable solvent effect that usually motivates variable coordination behaviors of metal cations, even in a same reaction system, which can modulate the coordination microenvironment and the geometric symmetry of the metallic core[32]. Herein, two monometallic erbium complexes, $[Er(bpad)_3]\cdot CH_3OH\cdot H_2O$ (**1**) and $[Er(bpad)_2(H_2O)_2]NO_3\cdot 3H_2O$ (**2**), have been isolated by changing the solvent ratio, with which the Er(Ⅲ) ion is surrounded, leading to a nona-coordinated monocapped square antiprism (C_{4v}) and octa-coordinated biaugmented trigonal prism (C_{2v}) geometries, respectively. In addition, the magnetic properties of complexes **1** and **2** have been investigated.

1 Experimental

1.1 Materials and methods

The Hbpad ligand was synthesized following a previous reference[33]. Other chemicals were reagent grade and commercially available. Fourier transform infrared (FT-IR) spectra were recorded in a range of 400~4 000 cm^{-1} using KBr pellets on an EQUINOX55 FT/IR spectrophotometer. Elemental analysis (carbon, hydrogen and nitrogen) was implemented on a PerkinElmer 2400 CHN analyzer. Magnetic measurements were accomplished using a Quantum Design MPMS-XL7 SQUID magnetometer on polycrystalline samples (restrained in eicosane to prevent torquing at high fields). The diamagnetic corrections for the complexes were estimated using Pascals constants.

1.2 Synthesis of $[Er(bpad)_3]\cdot CH_3OH\cdot H_2O$ (1)

A mixed CH_3OH/H_2O solution (15 mL, 2∶1, *V*/*V*) of triethylamine (0.007 mL, 0.05 mmol) and Hbpad (0.146 g, 0.6 mmol) was stirred for 1 h, and then $Er(NO_3)_3\cdot 6H_2O$ (0.091 g, 0.2 mmol) was added. The mixture above was allowed to be stirring for 5 h and shelved after filtration. Yellow crystals of **1** were isolated after 4 days (Yield: 72%, based on Er^{3+}). Anal. Calcd. for $C_{40}H_{39}ErN_{12}O_5$(%): C, 51.38; H, 4.20; N, 17.98. Found(%): C, 51.42; H, 4.25; N, 18.02. IR (KBr, cm^{-1}): 3 442 (w), 1 633 (m), 1 560 (s), 1 521 (s),

1 472 (s), 1 187 (s), 1 436 (m), 1 362 (s), 1 165(w), 1 029(w), 805 (w), 713 (m).

1.3 Synthesis of $[Er(bpad)_2(H_2O)_2]NO_3\cdot 3H_2O$ (2)

Complex **2** was prepared by the similar way of **1**, while the ratio of CH_3OH to H_2O is altered to be 1:2 (*V*/*V*). Pale yellow crystals of **2** were obtained after 5 days (Yield: 68%, based on Er^{3+}). Anal. Calcd. for $C_{26}H_{32}ErN_9O_{10}$(%): C, 39.14; H, 4.04; N, 15.80. Found (%): C, 39.18; H, 4.07; N, 15.75. IR (KBr, cm^{-1}): 3 436 (w), 1 635 (s), 1 585 (s), 1 565 (s), 1 521 (s), 1 479 (s), 1 436 (m), 1 393 (s), 1 168 (m), 1 063 (m), 912 (w), 743 (m), 710 (s).

1.4 Crystallographic data collection and refinement

Single-crystal X-ray diffraction data for complexes **1** and **2** were collected on a Bruker SMART APEX CCD diffractometer equipped with graphite-monochromated Mo $K\alpha$ radiation (λ=0.071 073 nm). Data processing and absorption corrections were accomplished using SAINT and SADABS[34]. The structures were solved by direct methods and refined against F^2 by full-matrix least-squares with SHELXTL program[35]. All non-hydrogen atoms were refined with anisotropic thermal parameters. All hydrogen atoms were positioned geometrically and refined using a riding model. Crystallographic data and refinement parameters are listed in Table 1, while selected interatomic distances and angles for complexes **1** and **2** are given in Table S1 (Supporting information).

CCDC: 1478582, **1**; 1478579, **2**.

Table 1　Crystallographic data and refinement parameters for 1 and 2

Complex	1	2
Empirical formula	$C_{40}H_{39}ErN_{12}O_5$	$C_{26}H_{32}ErN_9O_{10}$
Formula weight	935.09	797.87
Crystal system	Monoclinic	Monoclinic
Space group	*C*2/*c*	$P2_1/n$
a / nm	3.492 68(18)	0.885 17(8)
b / nm	1.158 68(8)	2.541 6(2)
c / nm	2.234 55(14)	1.428 89(13)
β / (°)	112.979(4)	105.107 0(10)
V / nm^3	8.325 4(9)	3.103 6(5)
Z	8	4
D_c / ($g\cdot cm^{-3}$)	1.492	1.708
μ / mm^{-1}	2.074	2.774
Crystal size / mm	0.21×0.20×0.19	0.30×0.25×0.13
Temperature / K	293	296
R_{int}	0.041 6	0.022 5
θ range / (°)	1.27~25.01	1.68~25.01
Total, unique reflection	20 903, 7 342	15 598, 5 471
Final *R* indices [$I>2\sigma(I)$]	R_1=0.036 3, wR_2=0.096 0	R_1=0.025 8, wR_2=0.056 3
R indices (all data)	R_1=0.061 1, wR_2=0.121 5	R_1=0.038 6, wR_2=0.063 0

2 Results and discussion

2.1 Crystal structure

X-ray determination suggests that both complexes are mononuclear structures. Complexes **1** and **2** belong to the monoclinic *C*2/*c* and $P2_1/n$ space groups, respectively. The Er(Ⅲ) site in the asymmetric unit of **1** is nona-coordinated by three O atoms and six N atoms from three tridentate $bpad^-$ ligands (Fig.1). The average Er-O and Er-N bond lengths are 0.236 1 and 0.254 6 nm, respectively(Table S1). The shortest Er⋯Er distance between neutral $[Er(bpad)_3]$ molecules is 0.955 9 nm. Being compared with **1**, a tridentate $bpad^-$ ligand are substituted by two coordinated H_2O

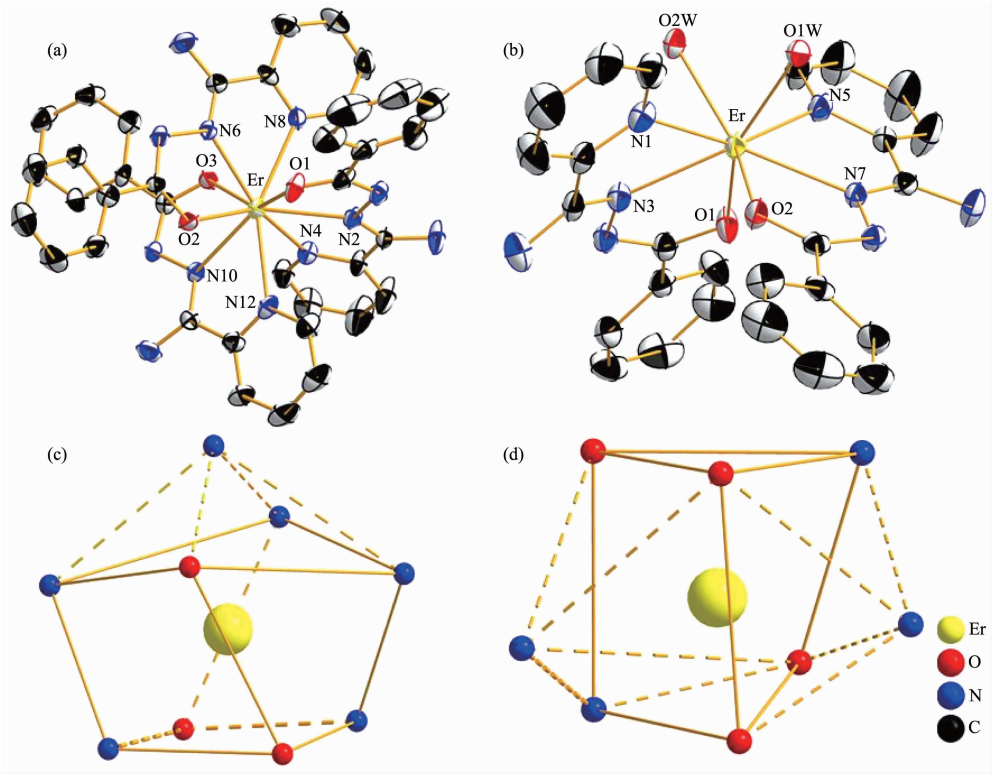

Hydrogen atoms and solvent molecules are omitted for clarity; Thermal ellipsoids are drawn at 50% probability

Fig.1 Crystal structures of **1** (a) and **2** (b) and local coordination geometries of the Er(Ⅲ) ions for **1** (c) and **2** (d)

molecules, forming the configuration of **2**. Accordingly, the metal center in **2** is bonded by two tridentate bpad$^-$ anions and two coordinated H_2O units, thus completing the ErN_4O_4 coordination group (Fig.1). The average Er-O and Er-N bond lengths are 0.236 5 and 0.247 3 nm, respectively. The closest Er⋯Er separation between two isolated molecules in **2** is 0.697 1 nm. Evidently, the steric hindrance of H_2O in **2** is far less than the bpad$^-$ ligand in **1**, giving rise to the shorter intermolecular distance in **2** compared to that in **1**. Hydrogen bonds and π-π interactions coexist in **1** and **2**, yielding a three-dimensional supramolecular structure (Fig.S1).

To ascertain the precise geometries around the metallic centers and the degree of the distortion from the ideal model for both complexes, the geometric spheres of Er(Ⅲ) cations are calculated by using the SHAPE 2.1 program[36] based on the structural parameters, and the typical geometric polyhedrons are depicted in Fig.1. As listed in Table S2, the calculated values illuminate that the Er(Ⅲ) ion in **1** is best described as a monocapped square-antiprism (C_{4v}) with moderate distortions from the ideal geometry. By contrast, the Er(Ⅲ) nodes in **2** represent a biaugmented trigonal prism (C_{2v}).

2.2 Magnetic studies

In order to understand the consequence of this ligand architecture on the local anisotropy of Er(Ⅲ) ion, magnetic susceptibility measurements were performed with a SQUID magnetometer on freshly prepared ground polycrystalline samples of **1** and **2** sealed under N_2 to prevent sample degradation. Direct current magnetic susceptibility measurements were conducted in a temperature range of 1.8~300 K under an applied dc field of 0.1 T (Fig.2). The room temperature $\chi_M T$ values of 11.58 and 11.37 cm^3·K·mol^{-1} for **1** and **2**, respectively, are in good agreement with the theoretical value of 11.48 cm^3·K·mol^{-1} for a mononuclear Er(Ⅲ) ($^4I_{15/2}$, S=3/2, L=6, g_J=6/5) complex. Upon decrease of the temperature, the $\chi_M T$ product remained nearly constant then decreased gradually between 100 and 50 K. Below 50 K, there was a

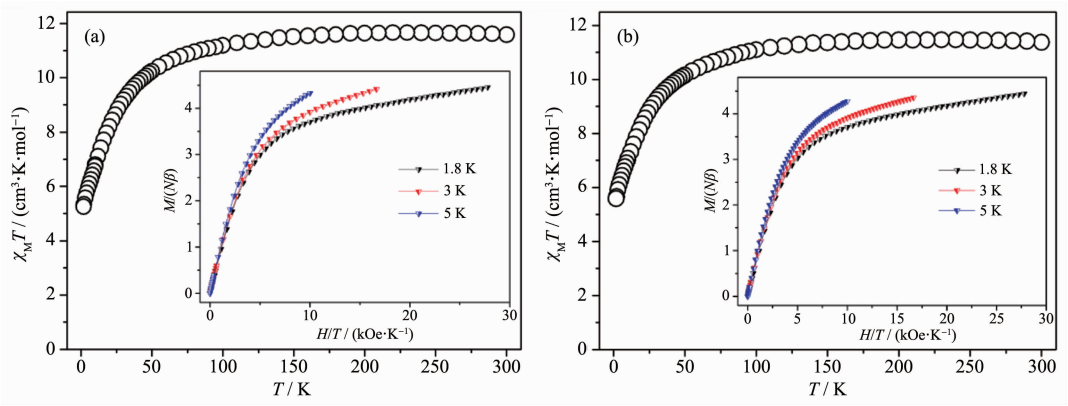

Inset: plots of M vs H/T at different temperatures

Fig.2　Plots of $\chi_M T$ vs T for **1** (a) and **2** (b)

sharp decrease reaching the minimums of 5.25 and 5.58 $cm^3 \cdot K \cdot mol^{-1}$ for **1** and **2** at 1.8 K, respectively. Such behavior is resulted from significant anisotropy as seen in some highly anisotropic complexes or weak antiferromagnetic dipolar coupling between the mononuclear groups[37-38]. Isothermal magnetization curves at 1.8 K exhibited saturation for **1** and **2** with values of 4.77$N\beta$ and 4.44$N\beta$ (Fig.S2), respectively, which prominently deviate from the saturated value of 10$N\beta$. The non-saturation as well as the non-superimposition of iso-temperature lines in the M vs H/T plot also confirm the presence of significant magnetic anisotropy in **1** and **2** (Fig.2, Inset). Therefore, alternating-current magnetic susceptibility measurements for complexes **1** and **2** were carried out under 0 dc field in a range of 1.8 ~20 K and a frequency of 1 000 Hz (Fig.S3). Unfortunately, no out-of-phase (χ_M'') signal was observed until the temperature dropped to 1.8 K, suggesting a fast quantum tunneling of magnetization (QTM) through the spin-reversal barrier and the inexistence of SMM behavior in the absence of extra field. To gain insight into the relationship between configuration and magnetic relaxation behavior, structural and magnetic parameters of some Er(Ⅲ) complexes are summarized in Table S3[23,39-47]. It is observed that the ligand field design plays a crucial role for the observance of SMM behavior in Er(Ⅲ) complexes. The sandwich-type ligand geometry leads to a higher symmetry environment around the Er(Ⅲ) sites, thus exhibiting a superior magnetic property. The case with low-coordinated Er(Ⅲ) center may also act as a potential candidate for high-performant SMMs. In contrast, the seven or eight coordinated Er ions adverse to the zero-field slow magnetic relaxation.

3　Conclusions

This work reports the synthesis of two mononuclear Er(Ⅲ) complexes by means of solvent effect and the characterizations of them. For **1**, the coordination geometry of Er(Ⅲ) core in N_6O_3 motif could be best identified as a monocapped square-antiprism (C_{4v}), while the configuration of Er(Ⅲ) ion in **2** is surrounded by a biaugmented trigonal prism (C_{2v}) with N_4O_4 group. Magnetic studies unveil that the performance of slow magnetic relaxation is absent in these systems, owing to the possible QTM which can usually be efficiently suppressed by a DC field. The related follow-up tests are under way. The impetus for the case presented herein is to exploit the potential of synthesizing Er-based single-molecule magnets, further studies following this guideline are in progress.

Supporting information is available at http://www.wjhxxb.cn

References:

[1] Ishikawa N, Sugita M, Ishikawa T, et al. *J. Am. Chem. Soc.*, **2003**,**125**:8694-8695

[2] Takamatsu S, Ishikawa T, Koshihara S, et al. *Inorg. Chem.*, **2007**,**46**:7250-7252

[3] Gatteschi D, Sessoli R, Villain J. *Molecular Nanomagnets*.

Oxford: Oxford University Press, **2006**.

[4] Christou G, Gatteschi D, Hendrickson D N, et al. *MRS Bull.*, **2000**,**25**:66-71

[5] Sessoli R, Gatteschi D, Caneschi A, et al. *Nature*, **1993**,**365**: 141-143

[6] Ishikawa N. *Polyhedron*, **2007**,**26**:2147-2153

[7] Woodruff D N, Winpenny R E P, Layfield R A. *Chem. Rev.*, **2013**,**113**:5110-5148

[8] LI Dong-Ping(李东平), WANG Qian(王倩), XIE Yi-Bu(谢一步), et al. *Chinese J. Inorg. Chem.*(无机化学学报), **2018**,**34**(8):1547-1554

[9] Liu X Y, Ma X F, Yuan W Z, et al. *Inorg. Chem.*, **2018**,**57**: 14843-14851

[10]Woodruff D N, Tuna F, Bodensteiner M, et al. *Organometallics*, **2012**,**32**:1224-1229

[11]Zhang P, Zhang L, Xue S F, et al. *Chin. Sci. Bull.*, **2012**,**57**: 2517-2524

[12]WANG Hui-Na(王慧娜), LIU Ying-Xin(刘颖昕), LI Rong(李荣), et al. *Chinese J. Inorg. Chem.*(无机化学学报), **2016**, **32**(2):343-350

[13]Rinehart J D, Long J R. *Chem. Sci.*, **2011**,**2**:2078-2085

[14]Sessoli R, Powell A K. *Coord. Chem. Rev.*, **2009**,**253**:2328-2341

[15]Rinehart J D, Fang M, Evans W J, et al. *J. Am. Chem. Soc.*, **2011**,**133**:14236-14239

[16]Guo F S, Day B M, Chen Y C, et al. *Science*, **2018**,**362**: 1400-1403

[17]Zhang P, Guo Y N, Tang J. *Coord. Chem. Rev.*, **2013**,**257**: 1728-1763

[18]Ma X F, Chen B B, Zhang Y Q, et al. *Dalton. Trans.*, **2019**, **48**:12622-12631

[19]GE Jing-Yuan(葛景园), CHEN Zhong-Yan(陈忠研), MA Jian-Ping(马建平), et al. *Chinese J. Inorg. Chem.*(无机化学学报), **2018**,**34**(9):1761-1767

[20]Kühne I A, Ungur L, Esien K, et al. *Dalton. Trans.*, **2019**, **48**:15679-15686

[21]Feng M, Lyu B H, Wang M H, et al. *Inorg. Chem.*, **2019**,**58**: 10694-10703

[22]Pedersen K S, Ungur L, Sigrist M, et al. *Chem. Sci.*, **2014**,**5**: 1650-1660

[23]Jiang S D, Wang B W, Sun H L, et al. *J. Am. Chem. Soc.*, **2011**,**133**:4730-4733

[24]Zhang X, Vieru V, Feng X, et al. *Angew. Chem. Int. Ed.*, **2015**,**54**:9861-9865

[25]Liu X Y, Li F F, Ma X H, et al. *Dalton. Trans.*, **2017**,**46**: 1207-1217

[26]MA Xiao-Hui(马晓慧), LI Fei-Fei(李菲菲), CEN Pei-Pei(岑培培), et al. *Chinese J. Inorg. Chem.*(无机化学学报), **2017**, **33**(9):1639-1648

[27]Cen P P, Zhang S, Liu X Y, et al. *Inorg. Chem.*, **2017**,**56**: 3644-3656

[28]Duan C W, Hu L X, Ma J L. *J. Mater. Chem. A*, **2018**,**6**: 6309-6318

[29]Ma X H, Liu Y, Song W M, et al. *Dalton. Trans.*, **2018**,**47**: 12092-12104

[30]SUN Lin(孙琳), LIU Huai-Xian(刘怀贤), ZHOU Hui-Liang(周惠良), et al. *Chinese J. Inorg. Chem.*(无机化学学报), **2015**,**31**(6):1207-1214

[31]Liu B, Zhou H F, Hou L, et al. *Inorg. Chem.*, **2016**,**55**:8871-8880

[32]Jiang Y, Brunet G, Holmberg R J, et al. *Dalton. Trans.*, **2016**,**45**:16709-16715

[33]van Koningsbruggen P J, Haasnoot J G, de Graaff R A G, et al. *Inorg. Chim. Acta*, **1995**,**234**:87-94

[34]Sheldrick G M. *SADABS, Program for Empirical Absorption Correction for Area Detector Data*, University of Göttingen, Germany, **1996**.

[35]Sheldrick G M. *SHELXS*-2014 and *SHELXL*-2014: *Program for Crystal Structure Determination*, University of Göttingen, Germany, **2014**.

[36]Llunell M, Casanova D, Cirera J, et al. *SHAPE, Ver.*2.1, University of Barcelona, Spain, **2013**.

[37]Rinehart J D, Fang M, Evans W J, et al. *Nat. Chem.*, **2011**,**3**: 538-542

[38]Zadrozny J M, Xiao D J, Atanasov M, et al. *Nat. Chem.*, **2013**,**5**:577-581

[39]Le Roy J J, Korobkov I, Murugesu M. *Chem. Commun.*, **2014**,**50**:1602-1604

[40]Ungur L, Le Roy J J, Korobkov I, et al. *Angew. Chem. Int. Ed.*, **2014**,**53**:4413-4417

[41]Le Roy J J, Ungur L, Korobkov I, et al. *J. Am. Chem. Soc.*, **2014**,**136**:8003-8010

[42]Meihaus K R, Long J R. *J. Am. Chem. Soc.*, **2013**,**135**: 17952-17957

[43]AlDamen M A, Clemente-Juan J M, Coronado E, et al. *J. Am. Chem. Soc.*, **2008**,**130**:8874-8875

[44]Xu W, Zhou Y, Huang D, et al. *Cryst. Growth Des.*, **2013**, **13**:5420-5432

[45]Pointillart F, Le Guennic B, Cauchy T, et al. *Inorg. Chem.*, **2013**,**52**:5978-5990

[46]Zhang P, Zhang L, Wang C, et al. *J. Am. Chem. Soc.*, **2014**, **136**:4484-4487

[47]Sun W B, Han B L, Lin P H, et al. *Dalton. Trans.*, **2013**,**42**: 13397-13403